17. Fang, J.-Y.; Guo, H. *J. Chem. Phys.* **1995**, *102*, 1944.
18. Bacic, Z.; Light, J. C. *J. Chem. Phys.* **1986**, *85*, 4594.
19. Light, J. C.; Hamilton, I. P.; Lill, J. V. *J. Chem. Phys.* **1985**, *82*, 1400.
20. Ratner, M. A.; Gerber, R. B. *J. Phys. Chem.* **1986**, *90*, 20.
21. Horn, T. R.; Gerber, R. B.; Ratner, M. A. *J. Chem. Phys.* **1989**, *91*, 1913.
22. Schatz, G. C.; Gerber, R. B.; Ratner, M. A. *J. Chem. Phys.* **1988**, *88*, 3709.
23. Neuhauser, D.; Judson, R. S.; Doury, D. J.; Adelman, O. E.; Shafer, N. E.; Kliner, A. V.; Zare, R. *Science* **1992**, *257*, 519.
24. Manopolous, D. E.; Stark, K.; Werner, H.-Y.; Arnold, D. W.; Bradforth, S. E.; Neumark, S. M. *Science* **1993**, *260*, 1605.
25. Gray, S. K.; Wozny, C. E. *J. Chem. Phys.* **1991**, *94*, 2817.
26. Waterland, R. L.; Lester, M. I.; Halberstadt, N. *J. Chem. Phys.* **1990**, *92*, 4261.
27. Seong, J.; Sun, H. *Bull. Korean Chem. Soc.* **1996**, *17*, 934.
28. Waterland, R. L.; Skene, J. M.; Lester, M. I. *J. Chem. Phys.* **1988**, *89*, 7277.
29. Beswick, J. A.; Delgado-Barrio, G. *J. Chem. Phys.* **1980**, *78*, 3653.
30. Gutmann, M.; Willberg, D. M.; Zewail, A. H. *J. Chem. Phys.* **1992**, *97*, 8037.
31. Seong, J.; Sun, H.; Ratner, M. A.; Schatz, G. C.; Gerber, R. B., *J. Phys. Chem.* in press.
32. Willberg, D. M.; Gutamann, M.; Breen, J. J.; Zewail, A. H. *J. Chem. Phys.* **1992**, *96*, 198.
33. Garcia-Velar, A. *J. Chem. Phys.* **1996**, *104*, 1047.
34. Blazy, J. A.; DeKoven, B. M.; Rusell, T. D.; Levy, D. H. *J. Chem. Phys.* **1980**, *72*, 2439.

A Monte Carlo Simulation Incorporated with Genetic Algorithm for the Transition Deposition of LB Film of Fatty Acid

Jeong-Woo Choi*, Kyung Sang Cho, Won Hong Lee, Sang Baek Lee†, and Han Sup Lee‡

Department of Chemical Engineering, Sogang University, Seoul 121-742, Korea
†Department of Chemical Engineering, Cheju National University, Chejusi, Cheju 690-756, Korea
‡Department of Textile Engineering, Inha University, Incheon 402-751, Korea
Received December 4, 1997

A Monte Carlo simulation incorporated with the genetic algorithm is presented to describe the defect known as "transition from Y-to X-type deposition" of the cadmium arachidate Langmuir-Blodgett multilayer film. Simulation is performed based on the detachment models of XY-type deposition. The transition is simulated by introducing a probability of surface molecule detachment considering interaction between neighboring molecules. The genetic algorithm is incorporated into Monte Carlo simulation to get the optimum value of the probability factors. The distribution of layers having different thickness predicted by the simulation correlates well with the measured distribution of thickness using the small-angle X-ray reflectivity. The effect of chain length and subphase temperature on the detachment probability are investigated using the simulation. Simulation results show that an increase (or a decrease) of two hydrocarbon chain is roughly equivalent to the detachment probability to a temperature decrease (or increase) of 15 K.

Introduction

Up to date, the Langmuir-Blodgett (LB) film technique has been applied to the fabrication of nanoscale molecular thin films with optically, electronically, or biologically useful functional properties. Since the ordered structure of LB films exhibits the optical and electrical characteristics in the molecular level, LB film technique has been applied to the molecular electronic devices.[1-6] However, due to the defects during the deposition, it is difficult to obtain the desired films, which prevents the practical application of LB film technique. For long-chain fatty acids that have a long hydrophobic hydrocarbon alkyl chain ("tail") and hydrophilic carboxyl group ("head"), LB film deposition is comparatively easy by their strong head-head and tail-tail interaction.

Long-chain fatty acids form a monolayer at the air-water interface when they are spread. This floating monolayer is transferred onto a substrate by passing the substrate during the upward or downward passage through the air-water interface. The transfer ratio is defined as the ratio of the film-coated area of the substrate to the consumed area of the floating monolayer. In the Y-type deposition, the transfer ratio is the same on both upstrokes and downstrokes. Y-type film has a centrosymmetric or bilayer structure because of tail-to-tail and head-to-head deposition. On the contrary, if the monolayer is transferred only on downstrokes, this type of film is called as X type. It could be expected that X-type film have a non-centrosymmetric structure owing to head-to-

tail deposition. Even for some long-chain fatty acid, it has been observed that transfer ratio on the upstrokes decreases as the film thickness increases, which indicates the formation of defects. This phenomena have been known as XY-type deposition or a transition deposition from Y- to X-type deposition.[7,8] Characteristic of the XY-type film is that the film has a centrosymmetric structure like the Y-type film according to X-ray diffraction analysis despite the partial X-type deposition.[7] The mechanisms of the transition deposition from Y- to X- type have been investigated.[7-10] From a morphological point of view, the molecular overturning model[7] and molecular peeling model[8] were proposed. It was proposed that molecules detach during upstrokes and then the detached molecules finally return to the film by the reattachment or via the floating monolayer. Monte Carlo deposition simulation based on the detachment model using the triangular molecular matrix have been performed and structure and number distribution of deposited layers are calculated using the reflectivity profile of soft X-rays.[9] The detachment probability factors in that study are measured using trial and error method. The authors have been previously applied the small-angle X-rays with synchrotron radiation to measure the thickness and number distribution of layer of 39 times deposited cadmium arachidate LB film for the investigation of Y- to X- type transition.[10] Small-angle X-rays are commonly and widely used rather than soft X-rays.

In this study, a Monte Carlo simulation incorporated with genetic algorithm is done to evaluate the detachment mechanism and thickness distribution obtained by small-angle X-ray analysis. Hexagonal molecular matrix structure of CdA LB film is adopted based on the scanning tunneling microscopy image.[11] The genetic algorithm is incorporated Monte Carlo simulation to get the optimum values of the detachment probability. Various factors including temperature and chain length which affect the detachment probability are simulated.

Experimental

Cadmium arachidate (CdA), cadmium beheniate (CdB) and cadmium stearate (CdS) were purchased from Sigma Chemical Co (St. Louis, USA). LB films of CdS, CdA, CdB were prepared using a rectangular Langmuir trough (Type 611, Nima Tech., UK). The deionized ultrapure water (>18MΩ/cm) with 4×10^{-4} M $CdCl_2$ and 5×10^{-5} M $KHCO_3$ was used as a subphase. The pH of the subphase was 6.5 and the temperature was kept at 20 °C. The monolayer was transferred onto the silicon wafer substrate with bound two silicon wafers to expose only the polished side of the silicon wafer. The substrate was passed through the air-water interface 39 times. The drying time during each stroke was 1,000 sec. The surface pressure and dipping speed were kept to be 15 mN/m and 0.7 mm/min, respectively. Deposition of the measured sample was typically XY type as shown in Figure 1. The X-ray reflectivity was measured at the Beam Line 3C2, Pohang Accelerator Lab. (PLS) in Korea, using monochromatic synchrotron X-ray radiation (λ=1.608 Å) and the four circle goniometer. Beam Line structure at PLS is described elsewhere.[12] In the profile of reflectivity *vs.* or grazing angle (θ) of the small angle X-rays (Figure 2), angle intervals and damping out of the oscillation represents the average thickness and number distribution of layer.[10] From this oscillatory profile, the number distribution of layer was obtained (Figure 3a). The average

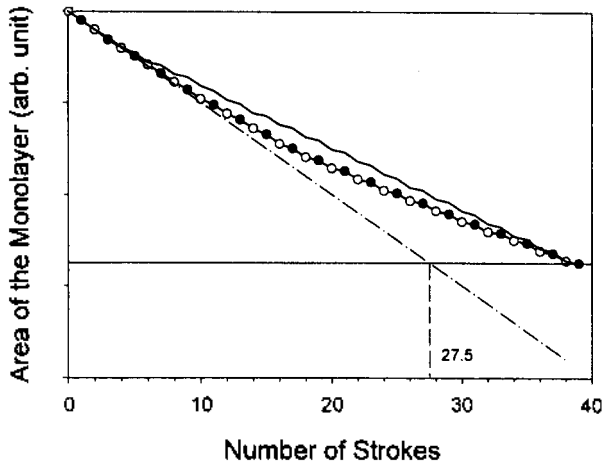

Figure 1. Measured consumption of the floating monolayer of cadmium arachidate after every stroke: ○→●, upstroke; ●→○, downstroke, -·-·-, Y-type deposition, —, simulation curve of monolayer consumption.

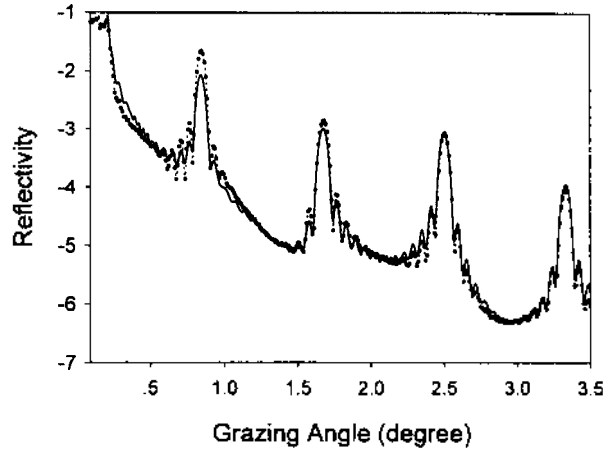

Figure 2. Reflectivity *vs.* θ of cadmium arachidate LB film: ···, measurement; —, calculation.

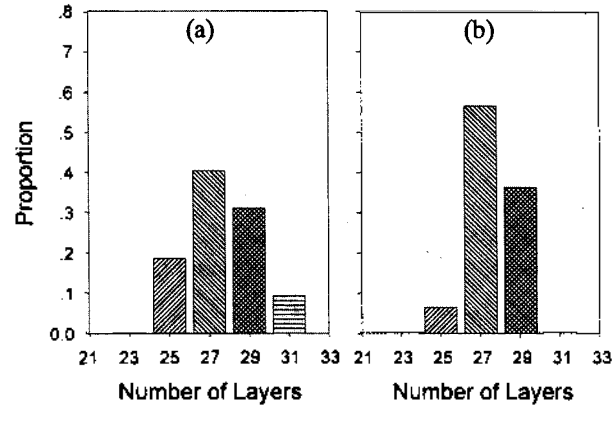

Figure 3. Number distribution of layer after the 39th stroke: (a) measurement using X-ray reflectivity; (b) simulation.

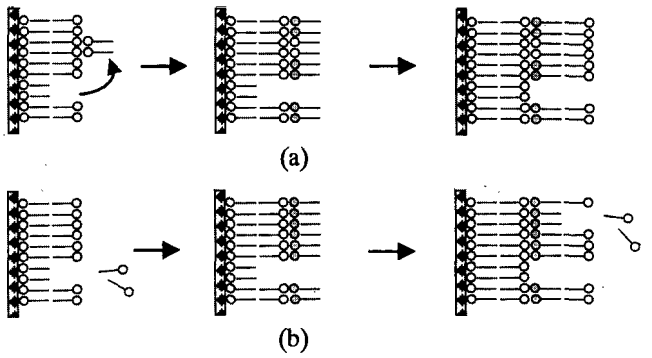

Figure 4. Models for detachment mechanism of XY-type LB film: (a) Honig's model; (b) Peng's Model.

number of layers was 27.6. Thus the thickness of the XY-type film was found to be inhomogeneous while the periodic structure of the film had not been deteriorated.

Simulation

Molecular detachment model. LB films can be fabricated owing to the attraction forces between hydrophobic headgroups and between hydrophilic tailgroups. The tailgroups are the non polar hydrocarbon chains and the interaction between tailgroups is a dispersion force. The interaction between tailgroups is relatively weaker than that between polar hydrophilic groups. So Y- to X-type transition can be occurred by the detachment of tail groups. Honig's molecular overturning model[7] and Peng's molecular peeling model[8] for XY-type deposition are shown in Figure 4. According to the Honig's model, in the subphase, some molecules detach, overturn and then re-attach to the film. In the Peng's model, it is assumed that lipid molecules peel off in the subphase and peeled molecules return to the float monolayer. Thus the morphological structure and consumed area of the monolayer expected by these two models cannot be distinguished.

Monte Carlo simulation incorporated with genetic algorithm. The detachment mechanism was simulated based on the Honig's and Peng's model. It is assumed that the required energy for detachment, E, can be described as[13]

$$E = E_0 - mE_1 \tag{1}$$

where E_1 is the interaction energy between neighboring molecules and E_0 is a binding energy in the absence of unoccupied site. m is the number of unoccupied first-nearest-neighboring site, Using E, detachment parameter, p, can be expressed as

$$p \propto \exp(-E/k_BT) \tag{2}$$

where k_B is the Boltzmann constant and T is the temperature of the subphase. From Eq. (1) and (2),

$$p = p_0 p_1^m \propto \exp(-E_0/k_BT)\exp(mE_1/k_BT) \tag{3}$$

where

$$p_0 \propto \exp(-E_0/k_BT)$$

and

$$p_1 \propto \exp(-E_1/k_BT)$$

The deposition process is simulated in 200×200 molecular matrix with periodic boundary condition. Based on the scanning tunneling microscopy image of CdA LB film,[11] hexagonal lattice structure was adopted, which makes m to be 6. Genetic algorithm was incorporated to find the optimum values of the detachment parameter (p_0, p_1) in the Monte Carlo simulation.

Genetic algorithm is a kind of optimization or search algorithm based on the natural selection and natural generation. It is stochastic search method based on the principles of three operations (reproduction, crossover and mutation) that is inspired by Darwinism evolution theory; a natural evolution of selection by fitness.[14] It represents the variables in searching into a binary code string which is referred to a chromosome. The detachment probability parameters (p_0, p_1) are encoded to the binary code strings to be used in the genetic algorithm. A population of chromosome are prepared and their performances are evaluated by actually applying these binary encoded parameters to the object system. The advantages using genetic algorithm as an optimization method are that mathematical equation or model are not involved by encoding parameters and a genetic algorithm is performed with a population of data which results in the avoidance of local minima problem. The measurement of performance is a real number which is referred to a fitness value. The fitness function can be described as

$$Fitness = \frac{K}{\sum_{i=1}^{n} |y_{set} - y_i| + (y_{set} - y_i)^2}. \tag{4}$$

where K is constant, and y_{set} and y_i are the set point value and measured value in the genetic algorithm, respectively. The overall process of Monte Carlo simulation incorporated

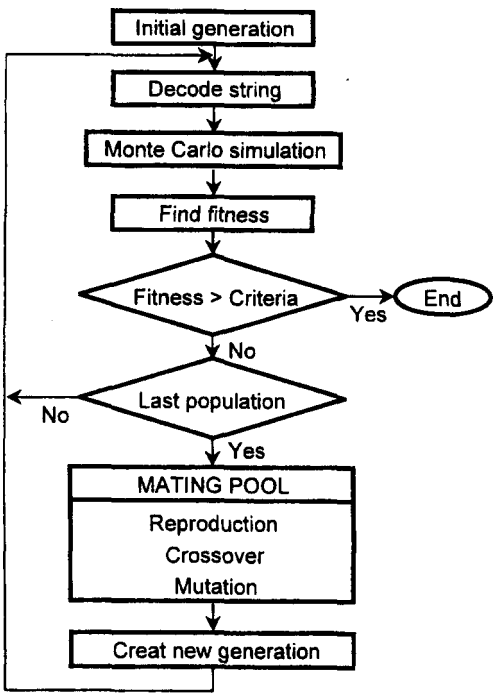

Figure 5. Overall procedure of Monte Carlo simulation incorporated with genetic algorithm.

with genetic algorithm is shown in Figure 5. Optimum p values can be chosen at the generation having the highest average fitness value with the restriction of the following two conditions. One condition was that the calculated average number of layers equaled the measured value. The other condition was that the difference in the transitional point from Y- to X-type deposition is minimized between the simulation and experimental measurement. Maximum and average fitness value were increased as the generation number increased during the Monte Carlo simulation incorporated with genetic algorithm as shown in Figure 6. p_0= 0.018, p_1=0.086 were obtained at 29th generation having the highest average fitness value.

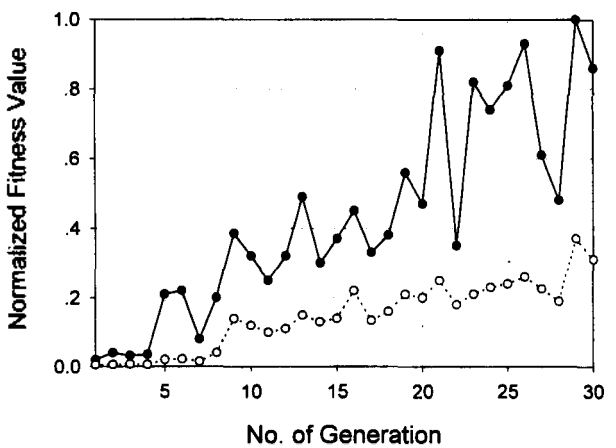

Figure 6. Fitness value of individual generation in simulation: ···○··· average fitness; —●— maximum fitness.

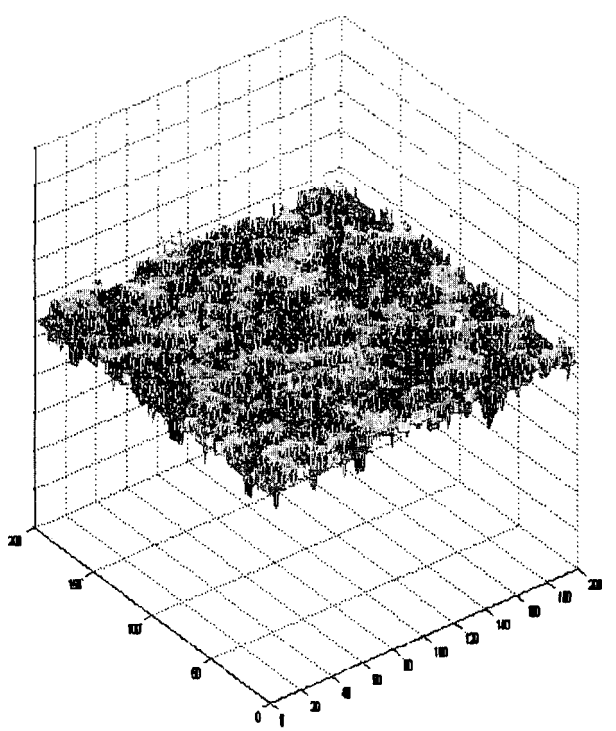

Figure 7. Simulation of surface appearance of cadmium arachidate LB film after 39th stroke with 200×200 matrix dimension. The 23rd, 25th, 27th, 29th and 31st layers are colored blue, light blue, green, orange and dark red.

Results and Discussion

Simulation result. Figure 1 shows the simulation result of the variation of consumed area during the deposition with p_0=0.018, p_1=0.086. The number distribution of layer can be obtained by simulation with the parameters of detachment probability calculated. The average number of layer obtained from the simulation is 27.6 layers. In this case, the portion of the 23, 25, 27, 29 and 31 layer are 0.2, 6.5, 56.7, 36.5, 0.1 percent, respectively. As shown in Figure 3, the number distribution of layer predicted by the Monte Carlo simulation corresponds well with that obtained from the small-angle X-ray analysis.[9] Figure 7 shows the surface appearance after the 39th stroke by the simulation. The 23rd, 25th, 27th, 29th and 31st layers are represented with different colors. The proportion of the each colored area to the entire area is shown in Figure 3b. The typical size of islands in Figure 7 is about 10 molecules.

Effect of chain length and subphase temperature. Figure 8(a) shows the consumed area of monolayer of CdS, CdA, CdB XY-type LB film during the 39 th strokes. Based on the transfer ratio, the average deposited layer were 26.4, 27.5 and 28.9 layer for CdS, CdA and CdB LB

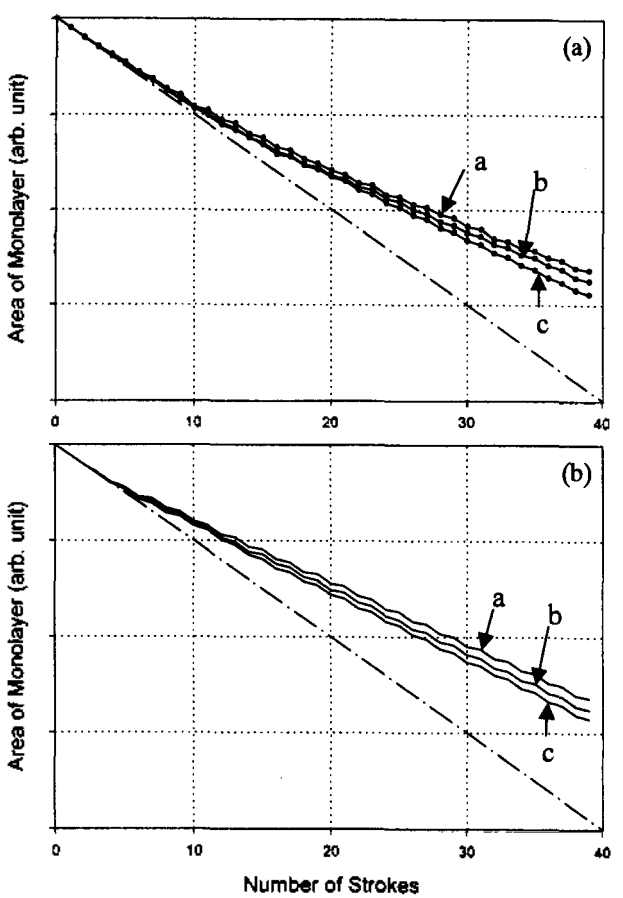

Figure 8. Consumption of floating monolayer after every stroke: (a) Measurement; (b) Simulation: curve a, cadminum stearate; curve b, cadmium arachidate; curve c, cadmium beheniate; – · – · –, Y-type deposition.

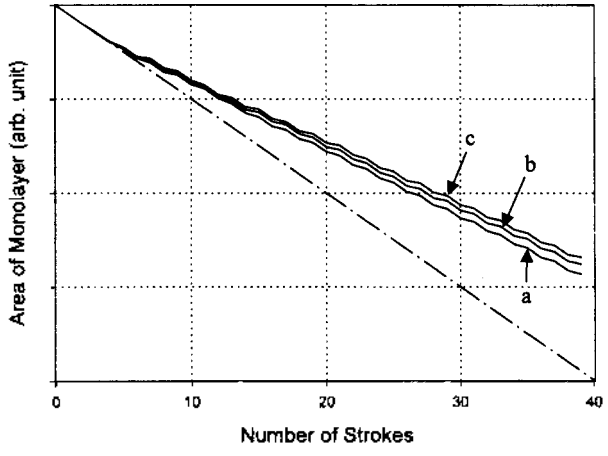

Figure 9. Simulation curve of monolayer consumption of cadmium arachidate: curve a, 278 K; curve b, 293 K; curve c, 318 K; - · - · -, Y-type deposition.

film, respectively. In the fatty acid LB film, the attraction force between tail group is mainly van der Waals force. In the non polar molecules, van der Waals force is proportional to the molecular weight. The detachment parameters calculated based on above relation are p_{0S}=0.024, p_{1S}=0.104, p_{0B}=0.014 and p_{1B}=0.073, respectively, where the subscript S and B represents the cadmium stearate and cadmium beheniate, respectively. Figure 8(b) shows the simulation results of the consumed area of the monolayer using the detachment parameters. The average deposited layer was 26.4, 27.6 and 28.6 for CdS, CdA and CdB LB film, respectively. The results of Monte Carlo simulation based on thermodynamic model correspond well with the experimental results. Figure 9 shows the effect of temperature on detachment probability of CdA LB film. The deposited layer at 278 K, 293 K and 308 K were 28.7, 27.6 and 26.8 layer, respectively.

Pallas and Pethica measured the π-A isotherms using n-pentadecanoic acid ($C_{14}H_{29}COOH$) and n-hexadecanoic acid ($C_{15}H_{31}COOH$) at 25 °C and 30 °C.[15] They revealed that an increase in temperature has increased the surface pressure of the phase transition form expanded to condensed phase and a decreases in the hydrocarbon chain length showed a similar result. Consideration of the force between the molecules in the floating monolayer can explain the above both effects. A decrease in the chain length makes van der Waals force between the molecules to be decreased, which results in cohesion reduction within the film. But a decrease in temperature causes less thermal motion, which results in less detachment of the molecules. As a rule porposed by Pallas and Pethica, reducing the hydrocarbon chain length of a long-chain fatty acid by one methylene group is roughly equivalent to a temperature increase of 5-10 K.[16] In this simulation, thermodynamic detachment probability factors considering the interaction (or binding) energy are adopted. Simulation results show that a increase of the number of methylene group of fatty acid and the reduction of the subphase temperature leads to less detachment of LB film. As a result, an increase (or a decrease) of 2 hydrocarbon chain is roughly equivalent to a temperature decrease (or increase) of 15 K, which well satisfies the rule of thumb.

Acknowledgment. This work was supported by the Research Fund on the Optical Technology Project (F-15, 1996) of the Korea Ministry of Science and Technology. The X-ray experiments at PLS, Korea, were supported by MOST and POSCO, Korea.

References

1. Ulman, A. *An Introduction to Ultrathin Films*; Academic Press: San Diego, CA, 1991.
2. Choi, J. W.; Jung, G. Y.; Oh, S. Y.; Lee W. H.; Shin, D. M. *Thin Solid Films* **1996**, *284/285*, 876.
3. Choi, J. W.; Kim, M. J.; Jung, S. W.; Oh, S. Y.; Lee, W. H.; Shin, D. M. *Mol. Cryst. Liq. Cryst.* **1996**, *280*, 367.
4. Choi, J. W.; Bae, J. Y.; Min, J.; Cho, K. S.; Lee, W. H. *Sensors and Materials* **1996**, *8(8)*, 493.
5. Choi, J. W.; Kim, M. J.; Jung, S. W.; Oh, S. Y.; Lee, W. H. Shin, D. M. *Mol. Cryst. Liq. Cryst.* **1997**, *294*, 217.
6. Choi, J. W.; Min, J.; Jung, J. W.; Rhee, H. W.; Lee, W. H. *Mol. Cryst. Liq. Cryst.* **1997**, *295*, 153.
7. Honig, E. P. *J. Colloid Interface Sci.* **1973**, *43*, 66.
8. Peng, J. B.; Ketterson, J. B.; Dutta, P. *Langmuir* **1988**, *4*, 1198.
9. Momose, A.; Hirai, Y.; Waki, I.; Imazakei, S.; Tomioka, Y.; Hayakawa, K.; Naito, M. *Thin Solid Films* **1989**, *178*, 519.
10. Choi, J. W.; Cho, K. S.; Rhee, H. W.; Lee, W. H.; Lee, H. S. Submitted to the Bulletin of the Korean Chemical Society 1997.
11. Braun, H. G.; Fuchs, H.; Shrepp, W. *Thin Solid Films* **1988**, *159*, 301.
12. Park, B. J.; Rah, S. Y.; Park, Y. J.; Lee, K. B. *Rev. Sci. Instrum.* **1995**, *66(2)*, 1722.
13. Momose, A.; Hirai, Y. *Thin Solid Films* **1991**, *204*, 175.
14. Hwang, H. S.; Woo, K. B. *J. of Fuzzy Logic and Intelligent System* **1989**, *2(3)*, 40.
15. Pallas, N. R.; Pethica, B. A. *Langmuir* **1985**, *1*, 509.
16. Petty, M. C. *Langmuir-Blodgett Film (an introduction)*; Cambridge University Press: Cambridge, GB, 1996.